J. Membrane Biol. 119, 199–210 (1991)
002226319100019V

The Journal of
Membrane Biology

Intracellular Potassium Activity and the Role of Potassium in Transepithelial Salt Transport in the Human Reabsorptive Sweat Duct

M.M. Reddy and P.M. Quinton
Division of Biomedical Sciences, University of California, Riverside, California 92521-0121

Summary. We have measured the intracellular potassium activity, $[K^+]_i$ and the mechanisms of transcellular K^+ transport in reabsorptive sweat duct (RSD) using intracellular ion-sensitive microelectrodes (ISMEs). The mean value of $[K^+]_i$ in RSD is 79.8 ± 4.1 mM (n = 39). Under conditions of microperfusion, the $[K^+]_i$ is above equilibrium across both the basolateral membrane, BLM (5.5 times) and the apical membrane, APM (7.8 times). The Na^+/K^+ pump inhibitor ouabain reduced $[K^+]_i$ towards passive distribution across the BLM. However, the $[K^+]_i$ is insensitive to the $Na^+/K^+/2\ Cl^-$ cotransport inhibitor bumetanide in the bath. Cl^- substitution in the lumen had no effect on $[K^+]_i$. In contrast, Cl^- substitution in the bath (basolateral side) depolarized BLM from −26.0 ± 2.6 mV to −4.7* ± 2.4 mV (n = 3; * indicates significant difference) and decreased $[K^+]_i$ from 76.0 ± 15.2 mM to 57.7* ± 12.7 mM (n = 3). Removal of K^+ in the bath decreased $[K^+]_i$ from 76.3 ± 15.0 mM to 32.3* ± 7.6 mM (n = 4) while depolarizing the BLM from −32.5 ± 4.1 mV to −28.3* ± 3.0 mV (n = 4). Raising the $[K^+]$ in the bath by 10-fold increased $[K^+]_i$ from 81.7 ± 9.0 mM to 95.0* ± 13.5 mM and depolarized the BLM from −25.7 ± 2.4 mV to −21.3* ± 2.9 mV (n = 4). The K^+ conductance inhibitor, Ba^{2+}, in the bath also increased $[K^+]_i$ from 85.8 ± 6.7 mM to 107.0* ± 11.5 mM (n = 4) and depolarized BLM from −25.8 ± 2.2 mV to −17.0* ± 3.1 mV (n = 4). Amiloride at 10^{-6} M increased $[K^+]_i$ from 77.5 ± 18.8 mM to 98.8* ± 21.6 mM (n = 4) and hyperpolarized both the BLM (from −35.5 ± 2.6 mV to −47.8* ± 4.3 mV) and the APM (from −27.5 ± 1.4 mV to −46.0* ± 3.5 mV, n = 4). However, amiloride at 10^{-4} M decreased $[K^+]_i$ from 64.5 ± 0.9 mM to 36.0* ± 9.9 mM and hyperpolarized both the BLM (from −24.7 ± 1.4 mV to −43.5* ± 4.2 mV) and APM (from −18.3 ± 0.9 mV to −43.5* ± 4.2 mV, n = 6). In contrast to the observations at the BLM, substitution of K^+ or application of Ba^{2+} in the lumen had no effect on the $[K^+]_i$ or the electrical properties of RSD, indicating the absence of a K^+ conductance in the APM. Our results indicate that (*i*) $[K^+]_i$ is above equilibrium due to the Na^+/K^+ pump; (*ii*) only the BLM has a K^+ conductance; (*iii*) $[K^+]_i$ is subject to modulation by transport status; (*iv*) K^+ is probably not involved in carrier-mediated ion transport across the cell membranes; and (*v*) the RSD does not secrete K^+ into the lumen.

Key Words sweat duct · K^+ transport · K^+-sensitive microelectrodes · amiloride · ouabain · barium

Introduction

Intracellular potassium activity, $[K^+]_i$ and cell membrane K^+ conductances play an important role in the transepithelial ion transport and the regulation of a variety of physiological functions [4]. However, there are wide differences among various epithelia with regard to (*i*) the intracellular K^+ activity [1, 7, 17], (*ii*) the mechanisms responsible for $[K^+]_i$ accumulation such as the Na^+/K^+ pump and KCl cotransport [1, 18], and (*iii*) the K^+-conductance properties of apical and basolateral membranes [12, 20]. Until now there has been almost no information available on the $[K^+]_i$, mechanism(s) of K^+ uptake, or the role of K^+ transport in the transepithelial salt movement of human reabsorptive sweat duct (RSD). In addition, RSD is a unique tissue compared with many NaCl absorbing epithelia, such as frog skin [13], gall bladder [11], and urinary bladder [7], in that the RSD has low cell membrane electrical potentials [24] and an extremely high transepithelial Cl^- conductance [22, 25, 26]. We do not know the physiological basis of such low cellular potentials [24], but several factors which could be responsible for the low potentials in RSD include (*i*) a very small ratio of transmembrane K^+ distribution ($[K^+]_i$ may be very low as compared to other epithelia), (*ii*) a small or absent K^+ conductance in the BLM[1] and

[1] Abbreviations: BLM = basolateral membrane; APM = apical membrane; V_b = electrical potential across the BLM; V_a = electrical potential across the APM; V_t = transepithelial potential; E_b = electromotive force across BLM; G_b^k = K^+ conductance of BLM; E_k = K^+ equilibrium potential; $\Delta E_b^k = E_k - V_b$ = driving force for K^+ across BLM; $\Delta E_a^k = E_k - V_a$ = driving force for K^+ across APM; $[K^+]_i^m$ = measured intracellular K^+ activity; $[K^+]_b^{Eq}$ = calculated $[K^+]_i$ for passive distribution across BLM for the value of V_b; and $[K^+]_a^{Eq}$ = calculated $[K^+]_i$ for passive distribution across APM for the value of V_a.

APM, (*iii*) membrane electromotive force (EMF) is generated by an ion other than K^+ (possibly Cl^-), and (*iv*) a large paracellular current loop in the RSD which shunts a more negative K^+-EMF across the BLM to a more positive apical EMF [24–26].

Any one of the above explanations could have significant physiological implications. For example, the magnitude of the K^+ electromotive force (E_k) at the BLM (which is a function of both the relative K^+ conductance and the ratio of transmembrane K^+ distribution) could influence not only the driving force for Cl^- exit across the BLM, but also the driving force for Na^+ entry across the APM due to a paracellular current loop and resultant voltage drop across the APM. In essence, the K^+ conductance and transcellular K^+ distribution can exert significant influence on the transepithelial salt transport [4]. We, therefore, sought to know the transmembrane distribution of K^+ and the K^+ conductance properties of the APM and BLM in order to understand the mechanism(s) involved in generating membrane electrical potentials which provide the driving forces for transepithelial salt transport.

We also hope to use this information on $[K^+]_i$ and K^+ transport properties of cell membranes to address another hitherto unanswered, but important question. Human sweat is always hypertonic in its K^+ concentration [2], but the source of hypertonic $[K^+]$ in the sweat is unknown. K^+ may be secreted hypertonically into the primary sweat by the secretory coil or into the lumen by the RSD as in the collecting tubule [20]. Using intracellular K^+-sensitive double-barreled microelectrodes, we have obtained data on $[K^+]_i$ and factors which influence cellular K^+ uptake and some of the K^+-conductance properties of the apical and basolateral membranes. This data provide insights into the role of K^+ in setting the membrane potentials of the RSD and into the source of K^+ in final sweat.

Materials and Methods

The methods for obtaining skin plugs from human subjects, dissection of sweat glands, and cannulation of RSD for electrophysiological studies are the same as described earlier [21, 24]. In short, the skin biopsies were obtained from human subjects after giving informed consent. The sweat glands were dissected from the biopsied skin plugs in Ringer's solution. RSDs of about 0.5 to 1.0 mM were isolated from the sweat gland by microdissection under visual control using a dissection microscope. The RSDs were transferred to a microperfusion chamber containing Ringer's solution for cannulation and perfusion. Prior to cannulation, the RSDs were maintained in cold Ringer's solution (5°C). All experiments were performed at 35 ± 2°C.

Double-barreled boroscilate glass capillaries (Clark Biomedical Supplies, Reading, England) were used to pull fine-tipped microelectrodes using a Flaming Brown microelectrode puller, model P-80 PC. While applying nitrogen gas pressure into one barrel (reference side), a drop of silazine substance (either Hexamethyl disilazane, Sigma, or N,N-dimethyltrimethylsilylamine, Fluka) was introduced into the neck of the second barrel using a Hamilton needle. The electrode was then baked inside a hot filament of 400–420°C for 15 min while maintaining the nitrogen pressure in the reference barrel. The tip of the silanized barrel was backfilled with a liquid K^+ exchanger (Corning). The electrode was backfilled with 200 mM KCl to the exchanger column. The reference electrode (nonsilanized barrel) was filled with 1 M Mg acetate (pH 7.4). After removing the air bubbles, freshly chloridated Ag-Ag Cl_2 electrodes were introduced into both barrels and the upper ends of the electrodes were sealed with postal wax to ensure mechanical stability and to prevent evaporation of the electrolyte solution. The resistances of the ion-sensitive and reference electrodes were about 35 GΩ and 200 MΩ, respectively.

Determination of Slope, Selectivity of ISME and $[K^+]_i$

The ISMEs were calibrated to assess the selectivity properties of the ion exchanger. For this purpose, the selectivity of the ISME was determined by the fixed interference ion method [29, 30] using 3-, 12- and 60-mM KCl solutions with 150-mM NaCl background. The intracellular ion activity was actually determined by the empirical method [15] which takes into account possible interference from intracellular Na^+ on the ion signal. Solutions of 5, 30, 80, 100, and 120 mM KCl in NaCl concentrations such that $[Na^+] + [K^+] = 150$ mM, were used to calibrate each electrode. Electrodes with a slope of less than 48 mV/10-fold change in K^+ concentration were rejected. The selectivity coefficient of the Corning K^+ exchanger for Na^+ over K^+ was between 0.02 to 0.04.

Impalement of Cells

The cells were impaled using a piezoelectric hybrid stepper motor (PM 500-20 Frankenberger, West Germany). High impedance electrometer (WPI model FD223) with an input impedance of $10^{15}\Omega$ was used to measure the signals from the ion-sensitive electrodes. The tip potential artifacts were usually less than 4 mV and corrections were made accordingly. In general, the criteria for choosing the cells for experimentation were the same as described earlier [24] which included a rapid voltage deflection of the reference electrode (V_b), stable value for V_b (of at least −20 mV) and the ion signal for at least 2 min prior to experimental manipulations, and return of the reference and ion signal to the baseline value (±2 mV) after withdrawal of the electrode from the cell.

Solutions

The composition of the Ringer's solutions used in the experiments (including ion substitution and pharmacological studies) is given in Table 1.

Table 1. The composition of various basic salt solutions (BSS) used in the experiments (the values are expressed as mM/liter)

	NaCl	HEPES	KH_2PO_4	K_2HPO_4	NaH_2PO_4	Na_2HPO_4	Ca^{2+}-acetate	$MgSO_4$	KCl	$BaCl_2$	NaGlu	Glucose
BSS (phosphate buffer) 50 mM K^+	150	—	0.38	2.1	—	—	1	1	—	—	—	10
BSS	104.6	—	0.38	2.1	—	—	1	1	45.4	—	—	10
0-K^+ BSS	150	—	—	—	0.38	2.1	1	1	—	—	—	10
0-Cl^- BSS	—	—	0.38	2.1	—	—	1	1	—	—	150	10
BSS (HEPES)	150	10	—	—	—	—	1	1	5	—	—	10
Ba^{2+}-BSS (HEPES)	150	10	—	—	—	—	1	1	5	5	—	10

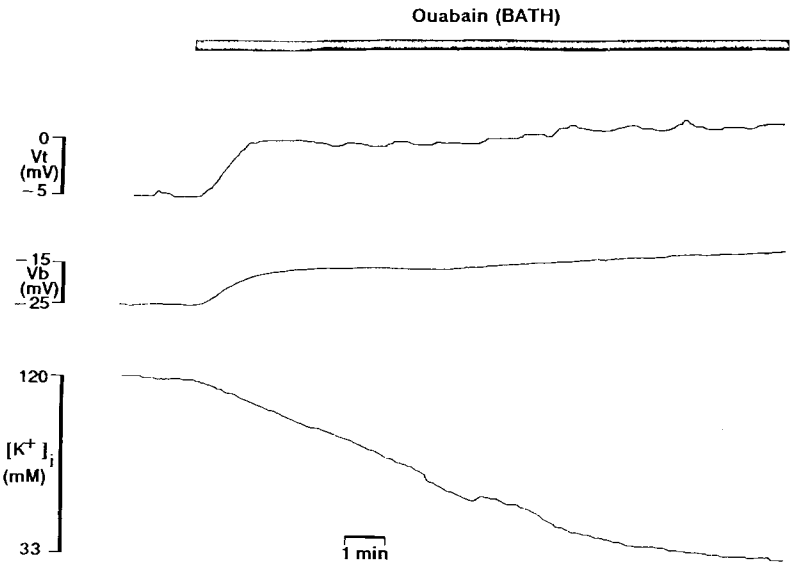

Fig. 1. Effect of Na^+/K^+ pump inhibition by ouabain on V_t, V_b and $[K^+]_i$. Notice that ouabain depolarized V_t and V_b and decreased $[K^+]_i$ towards equilibrium

Statistics

The data are tabulated and presented as the mean ± SE of the mean (where n = number of cells from a minimum of three human volunteer subjects). Statistical significance was determined on the basis of the Student's t test for paired samples when differences were evaluated for manipulations on the same cell. A P value of less than 0.05 was taken to be significantly different.

Results

$[K^+]_i$

The $[K^+]_i$ with normal Ringer's solution in the lumen and bath ranged from 37 to 125 mM with a mean value of 79.8 ± 4.1 mM (n (number of cells) = 39 from 16 subjects). The corresponding values of V_b and V_a measured with the reference side of the double-barreled electrode were −27.7 ± 0.9 mV and −18.8 ± 1.0 mV, respectively. The $[K^+]_i$ is above equilibrium both across the basolateral and apical membranes (Table 2). The ratio of $[K^+]_i$ measured, $[K^+]_i^m$ to the calculated value for a passive distribution, $[K^+]^{Eq}$ across cell membranes is 5.5 for BLM and 7.8 for the APM (Table 2).

Effect of Ouabain on $[K^+]_i$

Inhibition of Na^+/K^+ pump activity with ouabain in the bath depolarized the BLM from −24.7 ± 2.9 mV to −8.3* ± 3.6 mV (* indicates significant differences; $P > 0.05$) and decreased $[K^+]_i$ towards equilibrium (from 88.0 ± 16.0 mM to 16.0* ± 8.6 mM; $P > 0.05$; $n = 3$, Fig. 1). In two out of three measurements where we could hold the impalement for more than 24 min, the $[K^+]_i$ reached equilibrium across the BLM.

Table 2. Intracellular K^+ activity and its relationship with the electrical potential profile of microperfused (150 mM NaCl BSS in lumen/bath) RSD

V_t (mV)	V_a (mV)	V_b (mV)	$[K^+]_i^m$ (mM)	E_k (mV)	ΔE_b^k (mV)	ΔE_a^k (mV)	$[K^+]_b^{Eq}$ (mM)	$\frac{[K^+]_i^m}{[K^+]_b^{Eq}}$	$[K^+]_a^{Eq}$ (mM)	$\frac{[K^+]_i^m}{[K^+]_a^{Eq}}$
−8.9 ±0.8	−18.8 ±1.0	−27.7 ±0.9	79.8 ±4.1	−72.2[a]	44.5	53.4	14.5	5.5	10.3	7.8

$n = 39$.

[a] Since both lumen and contraluminal bath have equimolar K^+ concentration, the K^+ equilibrium potential (E_k) is similar at APM and BLM.

Table 3. Effect of 0-K^- in the bath on $[K^+]_i$ and the electrical properties of RSD

	V_t (mV)	V_a (mV)	V_b (mV)	$[K^+]_i^m$ (mM)	E_k (mV)	ΔE_b^k (mV)	ΔE_a^k (mV)	$[K^+]_b^{Eq}$ (mM)	$\frac{[K^+]_i^m}{[K^+]_b^{Eq}}$	$[K^+]_a^{Eq}$ (mM)	$\frac{[K^+]_i^m}{[K^+]_a^{Eq}}$
Control											
BSS (L)	−8.0	−24.5	−32.5	76.3	−71.0	38.5	46.5	14.9	5.1	12.8	6.0
BSS (B)	±1.3	±3.2	±4.1	±15.0							
Experimental											
BSS (L)	−2.8[a]	−25.5	−28.3[a]	32.3[a]	−132.6[b]	104.3	23.1	2.5[b]	12.9	13.3	2.4
0-K^+ BSS (B)	±1.1	±3.4	±3.0	±7.6							

$n = 4$.

[a] Significantly different from control. $P > 0.05$.

[b] The values are based on an assumed bath $[K^+]$ of 0.1 mM in an actually K^+-free BSS. E_k represents the value of potassium equilibrium potential across the BLM.

Apical Membrane K^+ Conductance

Zero mM K^+ in the lumen had no effect on V_a (V_a changed from a control value of -21.5 ± 3.2 mV to an experimental value of -22.0 ± 3.4 mV, $n = 4$) or $[K^+]_i$ ($[K^+]_i$ remained unchanged at 91.8 ± 13.6 mM, $n = 4$) even though there was a significant driving force for K^+ efflux across the apical membrane (137.7 mV, assuming 0.1 mM luminal $[K^+]$ in an actually 0-K^+ basic salt solution (BSS)). Application of Ba^{2+} to the luminal surface had no effect on the $[K^+]_i$ or V_a [23].

Effect of 0-K^+ (Bath) on $[K^+]_i$

Removal of K^+ from the bath resulted in a biphasic response of the V_b with an initial hyperpolarization and a subsequent depolarization of BLM followed by a gradual decrease in $[K^+]_i$. In about 15 min the removal of K^+ depolarized V_b from -32.5 ± 4.1 mV to $-28.3^* \pm 3.0$ mV while decreasing $[K^+]_i$ from 76.3 ± 15.0 mM to $32.3^* \pm 7.6$ mM ($n = 4$, $P > 0.05$, Table 3). The effects of 0 mM K^+ are reversible upon returning to the K^+-containing Ringer's solution. The apparent rate of K^+ efflux from the cell after exposure to 0-K^+ BSS in the bath is much slower (2.8 ± 0.7 mM/min, $n = 4$) than the apparent K^+ uptake after reintroducing K^+-containing BSS (11.3 ± 4.0 mM/min, $n = 4$). Within 2 min after reintroduction of K^+ in the bath, V_b underwent a transient undershoot to -52.5 ± 10.2 mV, $n = 4$ [23], but the mean $[K^+]_i$ during the transient peak of V_b was still below the levels of control $[K^+]_i$ (63.8 ± 13.3 mM).

Table 4. Effect of 50 mM K^+ in the bath on V_b and $[K^+]_i$ of RSD cells

	V_b	$[K^+]_i$
Control		
BSS (B)	−25.7	81.7
BSS (L)	±2.4	±9.0
Experiment		
50 mM K^+ (B)	−21.3[a]	95.0*
BSS (L)	±2.9	±13.5

$n = 4$.

[a] Significantly different from control. $P > 0.05$.

Effect of High K^+ in the Bath on $[K^+]_i$

Increasing the K^+ concentration by 10-fold in the bath depolarized the BLM by 4.4 mV while increasing the $[K^+]_i$ by about 13 mM ($n = 4$, Table 4).

Table 5. Effect of Ba^{2+} in the bath on the transcellular K^+ distribution in RSD

	V_t (mV)	V_a (mV)	V_b (mV)	$[K^+]_i^m$ (mM)	E_k (mV)	ΔE_b^k (mV)	ΔE_a^k (mV)	$[K^+]_b^{Eq}$ (mM)	$\frac{[K^+]_i^m}{[K^+]_b^{Eq}}$	$[K^+]_a^{Eq}$ (mM)	$\frac{[K^+]_i^m}{[K^+]_a^{Eq}}$
Control											
BSS (L)	−8.5	−17.3	−25.8	85.8	−74[b]	48.2	56.7	13.5	6.4	9.7	7.6
BSS-(HEPES) (B)	±1.3	±2.0	±2.2	±6.7							
Experimental											
BSS (L)	−6.7	−10.3	−17.0[a]	107.0[a]	−79.8[b]	62.8	69.5	9.6	11.2	7.4	16.5
Ba^{2+} BSS-(HEPES) (B)	±1.4	±2.6	±3.1	±11.5							

$n = 4$.

[a] Significantly different from the control. $P > 0.05$.

[b] Since the lumen and contraluminal bath contain equimolar K^+ concentrations, the E_k represents the value of K^+ equilibrium potential at APM and BLM.

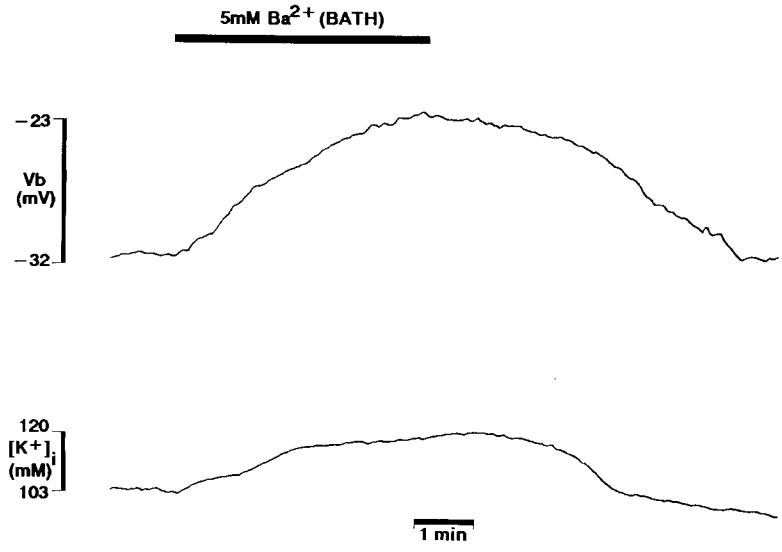

Fig. 2. Effect of K^+ conductance inhibitor Ba^{2+} on V_b and $[K^+]_i$. Notice that Ba^{2+} depolarized V_b and increased $[K^+]_i$. The effect of Ba^{2+} is completely reversible

Effect of Ba^{2+} on $[K^+]_i$

The K^+ conductance inhibitor, Ba^{2+}, depolarized the BLM by 8.8 mV ($n = 4$) within about 5 min while increasing the $[K^+]_i$ by 21.2 mM ($n = 4$). The driving force for K^+ efflux across the BLM (ΔE_b^k) increased from 48.2 to 62.8 mV (Table 5, Fig. 2).

Effect of Amiloride on $[K^+]_i$

Inhibition of Na^+ conductance with 10^{-6} M amiloride hyperpolarized both basolateral and apical membranes by 12.3 and 18.5 mV, respectively, while increasing the $[K^+]_i$ by 21.3 mM in about 5 min ($n = 4$, Table 6, Fig. 3).

In marked contrast to the effect of amiloride at 10^{-6} M, amiloride at a higher concentration (10^{-4} M) also hyperpolarized APM and BLM (Table 7, Fig. 4) and within about 1 min significantly reduced $[K^+]_i$ by 28.5 mM (≈19 mM/min, $n = 6$). Amiloride at this concentration significantly decreased the driving force for K^+ efflux across the BLM from 39.8 to 7.9 mV ($n = 6$, Table 7, Fig. 4).

Effect of Cl^- on $[K^+]_i$

Substitution of Cl^- by the impermeant anion gluconate in the lumen had no effect on $[K^+]_i$ although the driving force for K^+ efflux across the APM doubled within 1 min (ΔE_a^k changed from 59.3 to 115.6 mV). The APM depolarized by 55.8 mV ($n = 7$, Table 8, Fig. 5).

Substitution of Cl^- in the bath depolarized the BLM by 21.3 mV ($n = 3$) while decreasing $[K^+]_i$ by 18.4 mM ($n = 3$). In the absence of serosal Cl^-, the ΔE_b^k for K^+ efflux increased from 44.9 to 59 mV due to depolarization of the BLM (Table 9).

Table 6. Effect of 10^{-6} M amiloride in the lumen on the transcellular K^+ distribution in RSD

	V_t (mV)	V_a (mV)	V_b (mV)	$[K^+]_i^m$ (mM)	E_k (mV)	ΔE_b^k (mV)	ΔE_a^k (mV)	$[K^+]_b^{Eq}$ (mM)	$\frac{[K^+]_i^m}{[K^+]_b^{Eq}}$	$[K^+]_a^{Eq}$ (mM)	$\frac{[K^+]_i^m}{[K^+]_a^{Eq}}$
Control											
BSS (L)	−8.0	−27.5	−35.5	77.5	−71.4[b]	36.0	43.9	19.5	3.9	14.4	5.4
BSS (B)	±1.2	±1.4	±2.6	±18.8							
Experimental											
BSS + 10^{-6} M amiloride (L)	−1.8[a]	−46.0[a]	−47.8[a]	98.8[a]	−77.7[b]	29.9	31.7	31.3	3.2	29.2	2.6
BSS (B)	±0.8	±3.5	±4.3	±21.6							

$n = 4$.

[a] Significantly different from the control. $P > 0.05$.

[b] Since the lumen and contraluminal bath contain equimolar K^+ concentrations, the E_k represents the value of K^+ equilibrium potential at APM and BLM.

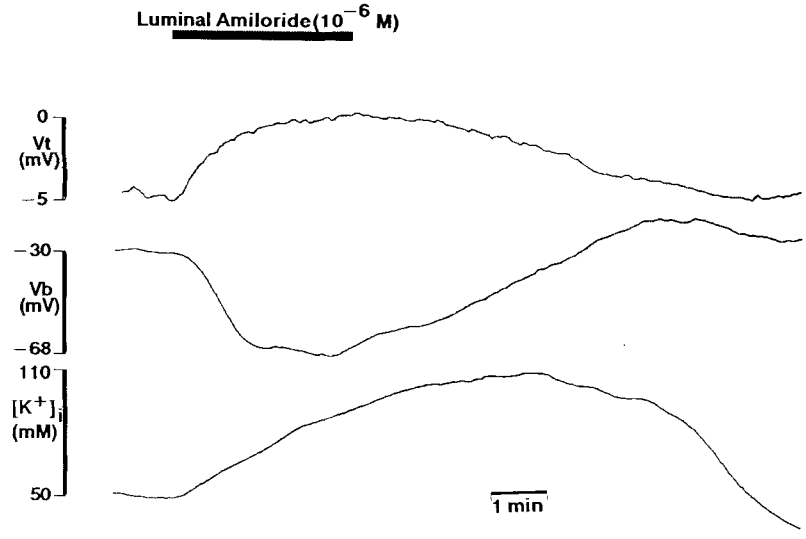

Fig. 3. Effect of Na^{2+} conductance inhibitor amiloride (10^{-6} M) on V_t, V_b and $[K^+]_i$. Notice that $[K^+]_i$ increased gradually following the application of luminal amiloride similar to the effect of Ba^{2+} in Fig. 2 and did not return to the baseline until after several minutes of amiloride washout even though V_b returned to the control value following the removal of amiloride

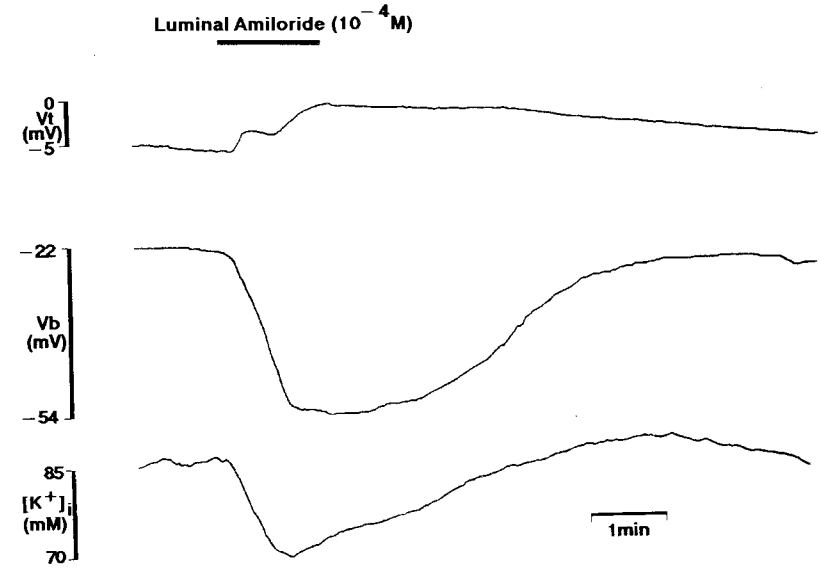

Fig. 4. Anomalous effect of amiloride at higher concentrations (10^{-4} M) on $[K^+]_i$. Notice that $[K^+]_i$ decreased rapidly following the application of amiloride to the luminal surface which returned to the baseline upon washout of amiloride

Table 7. Effect of 10^{-4} M amiloride in the lumen on the transcellular K^+ distribution in RSD

	V_t (mV)	V_a (mV)	V_b (mV)	$[K^+]_i^m$ (mM)	E_k (mV)	ΔE_b^k (mV)	ΔE_a^k (mV)	$[K^+]_b^{Eq}$ (mM)	$\frac{[K^+]_i^m}{[K^+]_b^{Eq}}$	$[K^+]_a^{Eq}$ (mM)	$\frac{[K^+]_i^m}{[K^+]_a^{Eq}}$
Control											
BSS (L)	−6.3	−18.3	−24.7	64.5	−66.6[b]	41.9	48.3	12.9	5.0	10.0	6.5
BSS (B)	±0.9	±0.9	±1.4	±0.9							
Experimental											
BSS + 10^{-4} M amiloride (L)	0.0[a]	−43.5[a]	−43.5[a]	36.0[a]	−51.4[b]	7.9	7.9	26.5	1.4	26.5	1.4
BSS (B)		±4.2	±3.9	±9.9							

$n = 6$.

[a] Significantly different from the control. $P > 0.05$.

[b] Since the lumen and contraluminal bath contain equimolar K^+ concentrations, the E_k represents the value of K^+ equilibrium potentials at APM and BLM.

Table 8. Effect of Cl^- substitution in the lumen on the $[K^+]_i$ of RSD

	V_t (mV)	V_a (mV)	V_b (mV)	$[K^+]_i^m$ (mM)	E_k (mV)	ΔE_b^k (mV)	ΔE_a^k (mV)	$[K^+]_b^{Eq}$ (mM)	$\frac{[K^+]_i^m}{[K^+]_b^{Eq}}$	$[K^+]_a^{Eq}$ (mM)	$\frac{[K^+]_i^m}{[K^+]_a^{Eq}}$
Control											
BSS (L)	−12.6	−13.4	−26.0	81.9	−72.7[b]	46.7	59.3	13.5	6.1	8.4	9.8
BSS (B)	±2.8	±2.3	±1.0	±9.9							
Experimental											
0-Cl BSS (L)	−80.6[a]	42.4[a]	−39.6[a]	82.1	+73.2[b]	33.6	115.6	22.8	3.6	1.0	82.1
BSS (B)	±4.6	±4.1	±1.8	±10.0							

$n = 7$.

[a] Significantly different from the control. $P > 0.05$.

[b] Since the lumen and contraluminal bath contain equimolar K^+ concentrations, the E_k represents the K^+ equilibrium potential across APM and BLM.

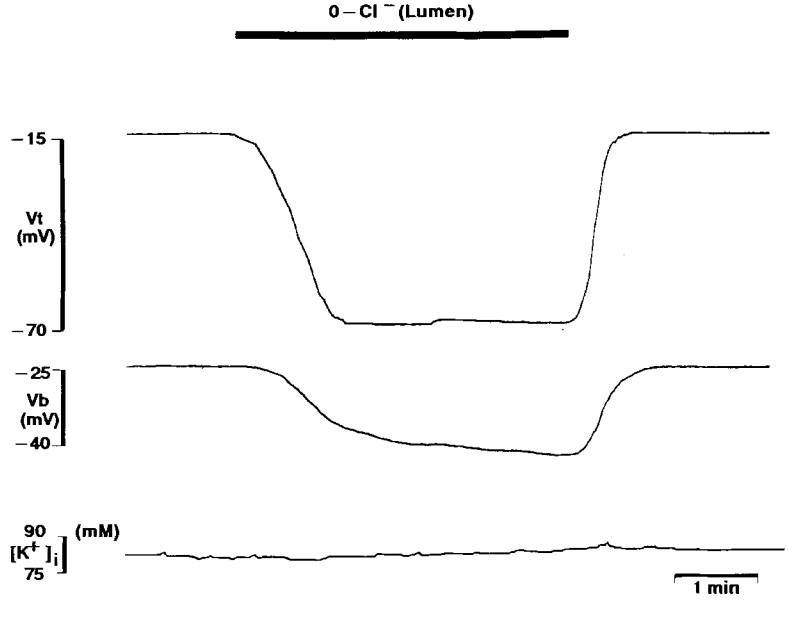

Fig. 5. Effect of Cl^- substitution in the lumen on V_t, V_b and $[K^+]_i$. Notice that removal of Cl^- from the lumen hyperpolarized V_t and V_b without any effect on $[K^+]_i$ although V_a was significantly depolarized (*see* Table 9)

Effect of Bumetanide

The $Na^+/K^+/2\ Cl^-$ cotransporter inhibitor bumetanide in the bath had no significant effect on the $[K^+]_i$ even at 10^{-3} M concentration. The $[K^+]_i$ in control conditions was 85.3 ± 7.5 mM as compared to 84.6 ± 6.8 mM ($n = 3$) in bumetanide for about 10 to 15 min.

Table 9. Effect of Cl^- substitution in the bath on the transcellular K^+ distribution in RSD

	V_t (mV)	V_a (mV)	V_b (mV)	$[K^+]_i^m$ (mM)	E_k (mV)	ΔE_b^k (mV)	ΔE_a^k (mV)	$[K^+]_b^{Eq}$ (mM)	$\frac{[K^+]_i^m}{[K^+]_b^{Eq}}$	$[K^+]_a^{Eq}$ (mM)	$\frac{[K^+]_i^m}{[K^+]_a^{Eq}}$
Control											
BSS (L)	−15.3	−10.6	−26.0	76.0	−70.9[b]	44.9	60.3	13.6	5.6	7.5	10.1
BSS (B)	±2.9	±5.2	±2.6	±15.2							
Experimental											
BSS (L)	11.0[a]	−15.7	−4.7[a]	57.7[a]	−63.7[b]	59.0	48	6.0	9.6	9.1	6.3
0-Cl BSS (B)	±0.6	±3.0	±2.4	±12.7							

$n = 3$.

[a] Significantly different from the control. $P > 0.05$.

[b] The concentration of K^+ is common to lumen and contraluminal bath. Therefore, E_k represents the K^+ equilibrium potential at APM and BLM.

Discussion

Critique of the Method

Although we had several cellular impalements with ISMEs with high membrane potentials similar to the values reported earlier the average steady-state values of cell potentials under control conditions were somewhat lower than previous measurements with conventional microelectrodes [24]. In order to minimize the impalement damage due to large tips of double-barreled electrodes, we would have preferred simultaneous dual impalement of cells (one reference and the other ISME). However, the technique is impractically difficult in RSD. On the other hand, double-barreled ISMEs offer a unique advantage in that both cell potential and ion activity are simultaneously monitored in the same cell. In addition, we believe the values of $[K^+]_i$ reported in this paper closely reflect actual values for several reasons. First, the values of $[K^+]_i$ were taken from stable impalements lasting from several minutes to more than an hour, so that the membrane should be tightly sealed with the electrode. Under these conditions the values of $[K^+]_i$ were either equal to or somewhat higher than the instantaneous $[K^+]_i$ values measured at the time of impalement (corresponding with the "injury" potential). We usually observed a postimpalement leak of $[K^+]_i$ but, within 2–4 min, the $[K^+]_i$ returned to a stable value which was similar to or larger than that at the time of impalement, indicating electrode sealing and reaccumulation of $[K^+]_i$ by the Na^+/K^+ pump. Second, the values of $[K^+]_i$ (Table 2) are similar to the values reported for other reabsorbing epithelia [6–8, 16, 28]. Third, since RSD appears to be a functional syncytium [14], the $[K^+]_i$ most likely reflects the mean $[K^+]_i$ of all the cells. Fourth, qualitatively, we did not find any difference in responses of V_b and $[K^+]_i$ between cells (within a wide range of V_b values between −20 to −40 mV) to any of the experimental manipulations, indicating that the conclusions drawn herein are not based on measurements in cells with erroneously low membrane potentials. The values of $[K^+]_i$ were uniformly low in cells from 2 out of 16 subjects which could not be attributed to the variation in the electrode size or shape. We retained the data from these subjects since we have no valid reason to exclude these data. Finally, the interference from intracellular $[Na^+]_i$ should be minimal because of high K^+ selectivity of the exchanger and minimal intracellular Na^+ (a maximum of 70 mM $[Na^+]_i$). Since we have used the empirical method of electrode calibration (with reciprocal dilution of Na^+ with K^+), any ambiguity in the Na^+ interference should be further minimized.

$[K^+]_i$

Our values of $[K^+]_i$ in the RSD are comparable to those reported for reabsorptive epithelia such as gall bladder [28], proximal tubules [8] and urinary bladder [7]. It is important to note that in all of the above epithelia, V_b is much closer to the K^+ equilibrium potential (E_k) across the BLM suggesting that in those epithelia the EMF at the BLM (E_b) is predominantly determined by transmembrane K^+ distribution. However, in RSD the V_b is much further removed from E_k (Table 2). The $[K^+]_i$ is accumulated in the cell against a large electrochemical gradient (Table 2) compared to many other reabsorbing epithelia [7, 8, 28]. The mechanisms involved in the accumulation of $[K^+]_i$ several times in excess of a passive distribution concentration are not understood. Several factors play a role in determining the value of $[K^+]_i$ such as Na^+/K^+ pump activity, $Na^+/K^+/2\,Cl^-$ or K^+/Cl^+ cotransporters at the APM and/or BLM and apical and basolateral membrane K^+

conductances. We have, therefore, investigated some of the factors which potentially determine the value of $[K^+]_i$.

Factors Responsible for Depletion and Accumulation of $[K^+]_i$

Na^+/K^+ Pump Activity and $[K^+]_i$

At first, we tested if the measured signal from the K^+ electrode is due to a change in the concentration of ions other than K^+ for which the electrode might be sensitive, which would overestimate $[K^+]_i$. However, when we inhibited Na^+/K^+ pump with ouabain, the transport was inhibited almost instantaneously ($V_t = 0$) and as expected, $[K^+]_i$ decreased towards equilibrium (Fig. 1) showing that Na^+/K^+ pump activity is mainly responsible for the K^+ accumulation in the cell and that our electrode is sensitive to $[K^+]_i$. The depolarization of the BLM due to pump inhibition is also consistent with the loss of K^+ from the cell due to ouabain. Since ouabain effects are rather slow to reverse in RSD, we further tested dependence of intracellular K^+ accumulation by removing K^+ from the bath, which reversibly inhibited the Na^+/K^+ pump (Table 3). Inhibition of pump activity by complete removal of K^+ in the bath depolarized the BLM and decreased $[K^+]_i$ towards equilibrium similar to the effects of ouabain. Although some of the loss of K^+ can be attributed to passive efflux of K^+ due to slightly increased driving force (ΔE_b^k) due to removal of extracellular K^+, inhibition of Na^+/K^+ pump is probably the main cause of depletion of $[K^+]_i$ [1]. Upon reactivation of the pump by introducing K^+ into the bath, there was a rapid hyperpolarization of BLM with a significant undershoot of V_b [23] which is consistent with the activation of Na^+/K^+ pump activity as was observed in the proximal tubule [1]. A comparison of the apparent rate of decrease of $[K^+]_i$ during inhibition of Na^+/K^+ pump activity with the apparent rate of K^+ uptake during the activation of the pump as reflected by changes in $[K^+]_i$ reveals that the rate of efflux of K^+ due to K^+ removal from the bath is about four times slower than the rate of active uptake of K^+ due to the reintroduction of K^+ into the medium [23] which is compatible with rapid activation of the Na^+/K^+ pump activity in the BLM. Part of the differences in the kinetics of $[K^+]_i$ during inhibition and reactivation of the Na^+/K^+ pump could be due to cell swelling (during inhibition of the Na^+/K^+ pump) and shrinking (during reactivation of the Na^+/K^+ pump). However, as judged by the relatively constant luminal and duct diameters, we did not notice any changes in cell volume during our measurements. These results indicate that Na^+/K^+ pump activity in the BLM is mainly responsible for the high $[K^+]_i$ values in the RSD, but does not exclude the role of other transport carriers such as $Na^+/K^+/2\ Cl^-$ or K^+/Cl^- cotransporters which in turn depend on the Na^+/K^+ pump activity [10].

Role of K^+-Dependent Cotransporter in the Intracellular K^+ Accumulation

In a number of reabsorptive epithelia it has been shown that K^+-dependent cotransporter (such as K^+/Cl^- and $Na^+/K^+/2\ Cl^-$) in the APM [9, 18] and/or BLM [11, 12, 27] contributes to transepithelial salt transport. Consequently, during the course of salt reabsorption, the K^+ cotransporters could either increase or decrease the $[K^+]_i$. Under the experimental conditions (150 NaCl in the lumen and bath) we found no evidence for a K^+ cotransporter. Neither substitution of luminal Cl^- (Fig. 5, Table 8) nor removal of K^+ from the lumen [23] had any effect on $[K^+]_i$. If a K^+ cotransporter were involved in salt transport across the APM, luminal substitution of Cl^- or K^+ should have decreased $[K^+]_i$. The absence of an effect of K^+ and Cl^- substitutions on $[K^+]_i$ suggest that a cotransporter does not play a significant role in the salt transport across the APM.

We do not have any evidence of a K^+-dependent cotransporter at the BLM either. Although removal of K^+ or Cl^- from the bath decreased $[K^+]_i$, the K^+ cotransport inhibitor bumetanide had no effect on $[K^+]_i$ even at a concentration of 10^{-3} M (*see* Results). These results indicate that the decrease in $[K^+]_i$ during K^+ and Cl^- substitution in the bath (Tables 3 and 9) is probably due to inhibition of Na^+/K^+ pump and depolarization of V_b, respectively. Since we do not have convincing evidence for a carrier-mediated K^+ transport process at the APM and BLM, we investigated the role of K^+ conductance in each cell membrane as a source of K^+ leak to balance the cellular loading of K^+ by the Na^+/K^+ pump.

Absence of K^+ Conductance in the APM

The APM in RSD does not seem to possess a K^+ conductance [3]. Imposition of a K^+ gradient by K^+ substitution in the lumen did not have any effect on the $[K^+]_i$ or on the electrical properties of the RSD [23]. Further, application of Ba^{2+} in the lumen did not affect $[K^+]_i$ [23]. By comparison, both of these manipulations in the bath had a significant effect on the BLM potential (Tables 3 and 5, Fig. 2). Further, if the APM has K^+ conductance, experimental manipulation of $[K^+]_i$ should affect V_a. When we decreased $[K^+]_i$ by substituting K^+ in the bath we

noticed a significant decrease in $[K^+]_i$ without a significant effect on V_a (Table 3) also suggesting that V_a is insensitive to changes in $[K^+]_i$ due to the absence of K^+ conductance in the APM. In contrast to our findings in RSD, several reabsorptive epithelia with amiloride-sensitive Na^+ conductance have a K^+ conductance in the APM [19, 20, 31–33]. Further, the urinary bladder [20] was reported to possess voltage-dependent K^+ conductance which is activated by depolarization of the APM. However, experimental depolarization of the APM by luminal Cl^- substitution did not affect $[K^+]_i$ either, although there is a significant driving force (ΔE_a^k) for K^+ exit across the APM (Table 8, Fig. 5), implicating the absence of K^+ conductance in the APM of RSD.

K^+ Conductance in the BLM

The low cell potentials in RSD [24] as compared to both the K^+ equilibrium potentials (Table 2) and the cell potentials of other epithelia [7, 28] seems to be due to a relatively low K^+ conductance rather than to an absence of K^+ conductance in the BLM based on several pieces of evidence. First, increasing the K^+ concentration 10-fold in the bath elevated $[K^+]_i$ and depolarized V_b (Table 4). Second, replacing the bath K^+ decreased $[K^+]_i$ with a transient hyperpolarization of V_b (Table 3, ref. [23]). Third, the K^+ conductance inhibitor Ba^{2+} increased $[K^+]_i$ and depolarized BLM (Table 5, Fig. 2). In addition, a K^+ conductance in the BLM should render $[K^+]_i$ sensitive to V_b. In fact, we have found that $[K^+]_i$ seems to be a direct function of V_b. Experimental depolarization of BLM by Cl^- substitution in the bath (Table 9) resulted in a dramatic decrease in $[K^+]_i$ probably due to the decrease in intracellular negativity which is consistent with G_b^k. Still, it is perplexing that in the presence of a significant G_b^k and a high E_k (Table 2), cell potentials in RSD are very low. These results suggest that either (*i*) the electromotive force (EMF) across the BLM (E_b) is not determined exclusively by K^+ distribution or (*ii*) that there is a significant paracellular shunt in the RSD that depolarizes E_b, away from E_k. However, we do have several indications which suggest that E_b in RSD is determined primarily by transmembrane Cl^- distribution. For example: (*i*) in RSD, 85% of the transepithelial conductance is due to Cl^- [22]; (*ii*) there is a significant Cl^- conductance in the BLM [25, 26] (*iii*) preliminary data from our laboratory on intracellular Cl^- activity revealed that the Cl^- equilibrium potential across the BLM is about -20 to -28 mV which is much closer to V_b; and (*iv*) a 10-fold change in K^+ concentration or inhibition of K^+ conductance with Ba^{2+} resulted in a much smaller depolarization (sub-Nernstian response) of V_b (Tables 4 and 5) indicating that a relatively small G_b^k is responsible for low values of V_b. Furthermore, in epithelia where V_b (and E_b) is primarily determined by a huge relative K^+ conductance in the BLM, G_b^k plays an active role in modulating the transepithelial salt transport [5]. However, in RSD, the role of relatively small G_b^k on transepithelial salt transport is unclear.

Properties of G_b^k and Transport

Amiloride

Inhibition of Na^+ conductance at the apical membrane by 10^{-6} M amiloride in the lumen increased $[K^+]_i$ while hyperpolarizing the BLM and APM. The increase in $[K^+]_i$ during inhibition of Na^+ transport suggests a possible decrease in G_b^k based on the following rationale. First, the increase in $[K^+]_i$ cannot be attributed to the increase in the Na^+/K^+ pump activity because a decrease in intracellular Na^+ (due to amiloride) should have decreased, not increased, the pump activity. Second, an increase in the holding potential for $[K^+]_i$ due to hyperpolarization of V_b (Table 6, Fig. 3) cannot be solely responsible for such a significant increase in $[K^+]_i$. Experimental hyperpolarization of V_b with luminal Cl^- substitutions (in some cases, the luminal Cl^- substitution hyperpolarized V_b as much as in the case of amiloride) did not increase $[K^+]_i$ (Table 8, Fig. 5), showing that hyperpolarization of V_b alone does not increase $[K^+]_i$. Third, blocking of G_b^k by Ba^{2+} caused a similar increase in $[K^+]_i$ (Table 5, Fig. 2). Fourth, in other amiloride-sensitive tight epithelia, G_b^k is reduced in parallel with decreasing the apical Na^+ conductance [5]. These observations indicate that the $[K^+]_i$ is not only a function of the Na^+/K^+ pump activity, but is also dependent on the transport status of Na^+ across the APM and the K^+ conductance across the BLM.

Anomalous Effects of Amiloride at Higher Concentration on $[K^+]_i$

Amiloride at a much higher concentration (10^{-4} M), decreased $[K^+]_i$. The effect is probably due to an increase in G_b^k (Table 7, Fig. 4) for the following reasons. First, the decrease in $[K^+]_i$ cannot be due solely to a decrease in Na^+/K^+ pump activity because the kinetics of change in $[K^+]_i$ due to inhibition of the Na^+/K^+ pump by ouabain or complete K^+ substitution in the bath are much slower as compared with the effect of amiloride (Figs. 1 and 4). Second, hyperpolarization of the BLM due to ami-

loride results in an increase in the holding potential for K^+ which favors K^+ influx, not efflux. In one experiment (*not shown*), the loss of K^+ due to amiloride (10^{-4} M) was, in fact, reduced by Ba^{2+} in the bath. Since amiloride has been used frequently at high concentrations in many epithelial ion transport studies as an inhibitor of Na^+ conductance, these observations stress the need for an awareness of possible nonspecific effects.

Effect of Transport Inhibition by Cl^- Substitution in the Lumen on G_b^k and $[K^+]_i$

Interestingly, in contrast to blocking Na^+ conductance, inhibition of Cl^- transport by luminal Cl^- substitution had little effect on the $[K^+]_i$ (Table 8, Fig. 5). Since $[K^+]_i$ is above equilibrium, an increase in G_b^k should have decreased $[K^+]_i$ as with 10^{-4} M amiloride (Table 7, Fig. 4) and vice versa, a decrease in G_b^k should have increased $[K^+]_i$ as in the case of Ba^{2+} (Table 5, Fig. 2). The fact that the $[K^+]_i$ is unchanged during Cl^- substitution in the lumen (Table 8, Fig. 5) indicates that the relationship between the G_b^k and the transport status at the apical membrane is mainly mediated by Na^+, but not Cl^- transport, at least within the duration of the experiment (about 4–6 min).

Some Implications of the Present Study

The K^+ concentration in the human sweat is much higher than in blood [2]. Our results indicate that there is no K^+ conductance or K^+-dependent carrier transport system to account for K^+ secretion across the APM. If there is any other K^+-dependent transporter such as Na^+/K^+ or K^+/H^+ exchange [2], substitution of K^+ in the lumen should have affected $[K^+]_i$. Since K^+ removal from the lumen had no effect on $[K^+]_i$ or on the electrical properties of RSD, a K^+-dependent carrier transport system probably does not exist in the APM. Further, the tight junctions of RSD appear to be impermeable to K^+ [3] indicating that a leak of K^+ into the lumen as a consequence of luminal negativity [21] is not a viable explanation either. Since K^+ concentration in sweat increases with decreased rates of sweat secretion [2], at low secretory rates NaCl and H_2O reabsorption may leave an excess of K^+ in the lumen. If this argument is to be accepted, inhibition of reabsorption should decrease K^+ hypertonicity in the sweat. However, in the sweat from cystic fibrosis (CF) subjects whose ductal reabsorption is impaired due to Cl^- impermeability [21], the K^+ concentration is significantly higher, not lower, than in the sweat from normal subjects [2]. These observations indicate that although reabsorption of water across a K^+-impermeable membrane as evidenced from the present studies may increase $[K^+]$ in the lumen to some extent, it is not the sole cause of K^+ accumulation in the lumen of RSD. It is, therefore, more likely that primary sweat from the secretory coil is the source of the higher K^+ concentrations in the sweat. Relatively higher K^+ concentration in the sweat from CF patients as compared to normals reflects another abnormality in the epithelial electrolyte transport in CF.

Conclusion

Our results indicate that $[K^+]_i$ in the RSD cell is above equilibrium and mainly due to the activity of the Na^+/K^+ pump in the BLM. There is neither a K^+ conductance nor a K^+-dependent transport in the APM. Only the BLM has a Ba^{2+}-sensitive K^+ conductance which can be modulated by the Na^+ transport status in the APM. Finally, the source of hypertonic K^+ in human sweat is probably the secretory coil and not the RSD.

We deeply appreciate the technical assistance of Kirk Taylor, Michael Ngo and Ruben Robles, as well as the secretarial assistance of Nancy Price, Debbie Vanderwater and Clarence Daniels. We also thank Dr. C. Bell for proofreading the manuscript. This work was supported by grants from the National Institute of Health, Bethesda, MD, DK 26547-11, the Getty Oil Co., the Gillette Co., Cystic Fibrosis Research Inc., and the U.S. National Cystic Fibrosis Foundation, R006 9-4.

References

1. Biagi, B., Sohtell, M., Giebisch, G. 1981. Intracellular potassium activity in the rabbit proximal straight tubule. *Am. J. Physiol.* **241:**F677–F686
2. Bijman, J., Quinton, P.M. 1984. Influence of abnormal Cl^- impermeability on sweating in cystic fibrosis. *Am J. Physiol* **247:**C3–C9
3. Bijman, J., Quinton, P.M. 1987. Permeability properties of cell membranes and tight junctions of normal and cystic fibrosis sweat ducts. *Pfluegers Arch.* **408:**505–510
4. Civan, M.M. 1980. Potassium activities in epithelia. *Fed. Proc.* **39:**2865–2870
5. Davis, C.W., Finn, A.L. 1982. Sodium transport inhibition by amiloride reduces basolateral membrane potassium conductance in tight epithelia. *Science* **216:**525–527
6. DeLong, J., Civan, M.M. 1978. Independence of cellular K^+ accumulation and net Na^+-transported by toad urinary bladder. *Fed. Proc.* **37:**569 (*Abstr.*)
7. DeLong, J., Civan, M.M. 1983. Microelectrode study of K^+ accumulation by tight epithelia: II. Effect of inhibiting transepithelial Na^+ transport on reaccumulation following depletion. *J. Membrane Biol.* **74:**155–164
8. Edelman, A., Curci, S., Samarzija, I., Fromter, E. 1978.

Determination of intracellular K^+ activity in rat kidney proximal tubular cells. *Pfluegers Arch.* **378:**37–45

9. Greger, R., Schlatter, E. 1983. Properties of the lumen membranes of the cortical thick ascending limb of Henle's Loop of rabbit kidney. *Pfluegers Arch.* **396:**315–324
10. Grinstein, S. 1986. Intracellular chloride concentration: Determinants and consequences. *In*: Genetics and Epithelial Cell Dysfunction in Cystic Fibrosis. J.R. Riordan and M. Buchwald, editors. pp. 31–43. Alan R. Liss, New York
11. Gunter-Smith, P.J., Schultz, S.G. 1982. Potassium transport and intracellular potassium activities in rabbit gallbladder. *J. Membrane Biol.* **65:**41–47
12. Halm, D.R., Krasney, E.J., Frizzell, R.A. 1985. Electrophysiology of flounder intestinal mucosa. 1. Conductance properties of the cellular and paracellular pathways. *J. Gen. Physiol.* **85:**843–864
13. Helman, S.J., Nagel, W., Fisher, R.S. 1979. Ouabain on active transepithelial sodium transport in frog skin. Studies with microelectrodes. *J. Gen. Physiol.* **74:**105–127
14. Jones, C.J., Quinton, P.M. 1989. Dye-coupling compartments in the human eccrine sweat gland. *Am. J. Physiol.* **256:**C678–C685
15. Jones, R.D.V., Aicken, C.C. 1987. Ion selective microelectrodes. *In*: Microelectrode Techniques. N.B. Standen, P.T.A. Gray, and M.J. Whitaker, editors. pp. 137–167. Company of Biologists, Cambridge
16. Kimura, G., Vrakabe, S., Yuasa, S., Miki, S., Takamitsu, Y., Orita, Y., Abe, H. 1977. Potassium activity and plasma membrane potentials in epithelial cells of toad bladder. *Am. J. Physiol.* **232:**F196–F200
17. Mortimer, C. 1978. Intracellular activities of sodium and potassium. *Am. J. Physiol.* **234:**F261–F269
18. Oberleithner, H., Greger, R., Neuman, S., Lang, F., Giebisch, G., Deetzen, P. (with the technical assistance of G. Geiger). 1983. Omission of luminal potassium reduces cellular chloride in early distal tubule of amphibian kidney. *Pfluegers Arch.* **398:**18–22
19. O'Neal, R.G., Sanson, S.C. 1984. Characterization of apical cell membrane Na^+ and K^+ conductances of cortical collecting duct using microelectrode techniques. *Am. J. Physiol.* **267:**F14–F24
20. Palmer, L. G. 1986. Apical membrane K^+ conductance in the Toad urinary bladder. *J. Membrane Biol.* **92:**217–226
21. Quinton, P.M. 1983. Chloride impermeability in cystic fibrosis. *Nature (London)* **301:**621–622
22. Quinton, P.M. 1986. Missing Cl^- conductance in cystic fibrosis. *Am. J. Physiol.* **251:**C649–C652
23. Quinton, P.M., Reddy, M.M. 1989. Cl^- conductance and acid secretion in the human sweat duct. *Ann NY Acad. Sci.* **574:**438–446
24. Reddy, M.M., Quinton, P.M. 1987. Intracellular potentials of microperfused human sweat duct cells. *Pfluegers Arch.* **410:**471–475
25. Reddy, M.M., Quinton, P.M. 1989. Altered electrical potential profile of human reabsorptive sweat duct cells in cystic fibrosis. *Am. J. Physiol.* **257:**C722-C726
26. Reddy, M.M., Quinton, P.M. 1989. Localization of Cl^- conductance in normal and Cl^- impermeability in cystic fibrosis sweat duct epithelium. *Am. J. Physiol.* **257:**C727–C735
27. Reuss, L. 1983. Basolateral KCl co-transport in a NaCl-absorbing epithelium. *Nature (London)* **305:**723–726
28. Reuss, L., Weinman, S.A., Grady, T.P. 1980. Intracellular K^+-activity and its relation to basolateral membrane ion transport in *Necturus* gall bladder epithelium. *J. Gen. Physiol.* **76:**33–52
29. Simon, W., Ammann, D., Oehme, M., Morf, W.E. 1978. Calcium-selective electrodes. *Ann. NY Acad. Sci.* **397:**52–69
30. Steiner, R.A., Dehme, M., Ammann, D., Simon, W. 1979. Neutral carrier sodium ion selective microelectrodes for intracellular studies. *Anal. Chem.* **51:**351–353
31. Stokes, J.B. 1984. Pathways of K^+ permeation across the rabbit cortical collecting tubule. *Am. J. Physiol.* **246:**F457–F466
32. Wills, N.K., Zeiske, W., van Driessche, W. 1982. Noise analysis reveals K^+ channel conductance fluctuations in the apical membrane of rabbit colon. *J. Membrane Biol.* **69:**187–197
33. Zeiske, W., Van Driessche, W. 1979. Saturable K^+ pathway across the outer border of frog skin (*Rana temporaria*): Kinetics and inhibition by Cs^+ and other cations. *J. Membrane Biol.* **47:**77–96

Received 28 February 1990; revised 20 August 1990